J. Sustain. Metall. (2017) 3:219–229
DOI 10.1007/s40831-016-0070-8

RESEARCH ARTICLE

Pyrometallurgical Treatment of High Manganese Containing Deep Sea Nodules

D. Friedmann[1] · A. K. Pophanken[1] · B. Friedrich[1]

Published online: 18 July 2016

Abstract The steadily growing demand for critical metals and their price increase on the world market makes the mining of marine mineral resources in the not too distant future probable. Therefore, a focus lays on the development of a sustainable, zero-waste process route to extract valuable metals from marine mineral resources such as manganese nodules. These nodules contain industrially important metals like nickel, copper and cobalt in substantial amounts. However, the development of a general metallurgical process route is challenging due to varying nodule compositions. Especially challenging is a high Mn content, since the liquidus temperature of a smelted slag phase directly correlates with Mn content. This paper presents thermodynamic models created in FactSage™ 6.4, which support direct reduction smelting of manganese nodules in an electric arc furnace. Thermodynamic modeling has never been applied to the metallurgical treatment of manganese nodules, and therefore, represents a significant advantage over previous studies. Furthermore, these calculations were verified in lab scale experiments. The nodules were supplied by BGR, German Federal Institute for Geosciences and Natural Resources, and have origin in the German licensed territory of the Clarion Clipperton Zone in the Pacific Ocean.

Keywords Marine mineral resources · Manganese nodules · Extractive metallurgy · Pyrometallurgy · Thermodynamic modeling

Introduction

The exploitation of manganese nodules from the deep sea has once again become a political and economic topic in recent years. Many countries have purchased exploration rights for territories in the Clarion Clipperton Zone south of Hawaii from the International Seabed Authority (ISA). The main focus of the processing of these nodules lays on the extraction of the industrial metals nickel, copper and cobalt. The nodules would serve as an enormous reserve for these metals, since they are found in relative abundance. For example, the nodules constitute an estimated reserve of up to 290 million tons of nickel and up to 60 million tons of cobalt. These estimated amounts currently surpass common land based reserves in mines for nickel, cobalt and manganese [1, 2]. Additionally, other valuable metals such as Molybdenum and Vanadium are found in relatively high concentrations. Thus, an extraction or at least enrichment in a marketable byproduct of these metals should also be pursued.

Background

Much of the current research builds on findings and results from the 1970s [3–7]. Herein, different approaches are studied. However, most research has only focused on hydrometallurgical approaches, since energy consumption to dry the 30–40 % moisture containing nodules is high. In the 1970s, four processes emerged, which were

The contributing editor for this article was Sharif Jahanshahi.

✉ D. Friedmann
dfriedmann@ime-aachen.de

[1] Department of Process Metallurgy and Metal Recycling (IME), RWTH Aachen University, Intzestraße 3, 52056 Aachen, Germany

considered viable to extract metal values from ocean nodules [8–11]:

(1) Reductive ammonia leach [12, 13]
(2) High-pressure sulfuric acid leach [14]
(3) Reduction and hydrochloric acid leach [15]
(4) Reductive smelting and sulfuric acid leach [16].

In the first process, an atmospheric ammonia-ammonium carbonate leach at 50 °C is employed. Manganese dioxide (MnO_2) is reduced to manganese oxide (MnO) or manganese carbonate ($MnCO_3$) using carbon-monoxide gas (CO). During the process cuprous ions (Cu^+) act catalytically, and therefore, have to be added to the leach liquor at a concentration of approximately 6 g/L [9]. This leaching step allows a recovery of about 90 % of the Ni and Cu content. However, only about 50 % of Co is recovered, since the iron matrix of the nodules, where Co substitutes Fe-Ions, is not attacked [10].

In the high-pressure acid leach process, the nodules are directly leached after grinding in an autoclave system at elevated temperatures (>180 °C) and a high oxygen partial pressure. After a retention time of one hour, a recovery of ~80 % Ni and ~90 % Cu is achieved. Recovery of Co content, however, is relatively low at approximately 50 % [17]. Yet, an explanation for this low recovery is not given.

The third process uses a high temperature hydrochlorination at 500 °C to yield water soluble chlorides and chlorine gas (Cl_2) following the chemical reaction exemplarily for manganese dioxide:

$$MnO_2 + 4\ HCl \rightarrow MnCl_2 + Cl_2 + 2\ H_2O \quad (1)$$

This process is characterized by the near complete dissolution of the mineral matrix, and therefore, shows very high metal recoveries greater 96 % for all valuable metals [18].

The fourth process is the only route, which employs pyrometallurgical extraction steps to treat manganese nodules. The process was developed by Sridhar et al. [16] of the former International Nickel Company (Inco) in 1976. A simplified flowchart of the process is depicted in Fig. 1. The studies presented by Sridhar et al. is the foundation for the research, which is discussed in this article. Thus, the process is evaluated more closely.

In the first step, the nodules are dried and pre-reduced in a rotary kiln. Here, the oxides of the valuable metals nickel, copper and cobalt are reduced at 1000 °C. 45 % of the iron content is also pre-reduced in this step. Ideally, the manganese content is only reduced to a lower oxidation state to crack the matrix, and therefore allow the extraction of valuable metals. In the following step, the preheated nodules are smelted without the addition of flux at 1380–1420 °C. On an industrial scale the smelting should be carried out in an electric arc furnace, but in their research Sridhar et al. simulated the smelting in a crucible

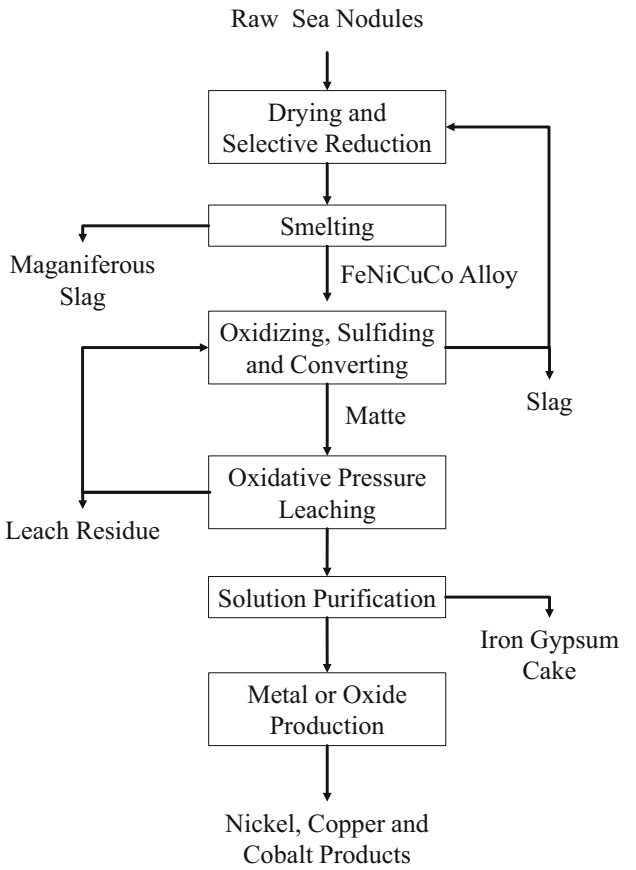

Fig. 1 Flowchart of the metal extraction process developed by Inco [16]

with small coal additions. Therefore, a direct adaptation of the research results to an industrially metallurgical treatment is arguable. In the smelting stage a 60–70 wt% Fe containing alloy is won. More than 95 % of the nickel, copper and cobalt are also reduced into this metal phase. The alloy only constitutes 6–8.5 % of the original dry nodule weight and is the intermediate product for the subsequent metal production.

Herein, lays the main advantage of the pyrometallurgical enrichment prior to the hydrometallurgical metal extraction, since downstream a far smaller amount of material has to be treated. Furthermore, these pre-enrichment steps result in a more economical and efficient leach solution production, because higher concentrations of metal values can be achieved [19]. An additional advantage of a smelting process is the possibility of a very efficient production of manganese or ferromanganese. This byproduct may easily be won from the manganiferous slag by further reduction at high temperatures (>1600 °C), whereas hydrometallurgical extraction routes only allow manganese recovery from a leach residue or as recrystallized Mn-salt with rather high energy consumption. Additionally, if Mn-recovery is not an objective, the slag would

be easier to dispose as acidic or alkaline leach residue [20]. Therefore, a pyrometallurgical approach for the treatment of nodules is more sustainable in terms of full resource use in comparison to hydrometallurgical options.

Direct leaching of the produced alloy, however, is not possible due to high acid consumption under enormous gas formation. Therefore, the alloy is further pyrometallurgically converted to remove iron. Silica (SiO_2) is added as flux and Fe is oxidized. The conversion is stopped at 5 wt% Fe to avoid high cobalt losses in the slag. The NiCu alloy obtained is then sulfided with elemental sulfur to produce a leachable matte. This matte is ground and leached with sulfuric acid ($\sim$1 mol/L) in an autoclave system at 110 °C and 1 MPa oxygen-pressure to avoid the formation of solid sulfur. The extraction rates in this step exceed 99 % [16]. Nevertheless, these stated values are arguable, since only synthetic mattes were leached during the studies.

The actual metal recovery in these four process routes is quite similar and subsequent processing are always hydrometallurgical steps, since pregnant leach liquors are obtained in all four processes. Nickel and copper are generally extracted by liquid ion exchange (LIX) using many different commercial organic solvents [9, 11] and after stripping into an aqueous phase obtained via electro winning (EW). Cobalt is often precipitated using hydrogen sulfide (H_2S) or also extracted by an organic solvent and subsequently electro won.

Nodule Composition and Implications

The nodules in this study origin are from the German licensed territory in the Pacific. In total 206 nodule samples were analyzed by ICP-OES and ICP-MS measurements. Table 1 shows that on average their manganese content is significantly higher than the nodule samples, studied earlier [9, 11, 14, 16]. The table further highlights that a metallurgical process to treat this kind of raw material has to be flexible in dealing with varying different nodule compositions. Therefore, a batch process would be ideal, since process parameters could be adjusted for each separate batch of nodules. The differing composition of the nodules studied here leads to a number of challenges:

1. Increased liquidus temperature of a slag phase
2. Resulting higher reduction temperature
3. Differing basicity of the slag
4. Increased energy requirements
5. Wear on furnace lining.

The main mineral phases of manganese nodules are complex, fine grained, often metastable, poorly crystallized and mostly nonstoichiometric [9]. Particle sizes vary, but are generally approximately 0.01 μm, highlighting why physical processing to enrich metal values is very difficult [1]. The most common minerals in ocean nodules are todorokite or 10 Å manganite (buserite), birnessite, vernadite and different iron oxides (mostly goethite and feroxyhyte) [9, 21].

A look at the quasi binary phase diagram of the main nodule constituents MnO, SiO_2, FeO, Al_2O_3 and MgO (Fig. 2) clearly illustrates how the ratio of MnO to SiO_2 significantly influences the liquidus temperature of the slag. This phase diagram was created using the "Phase Diagram" module of FactSage™. The diagram takes a constant fraction of FeO (12 wt%), Al_2O_3 (6 wt%) and MgO (5 wt%) into account. The resulting MnO/SiO_2 ratio is modeled as the x-axis. However, it should be noted that these five oxides do not represent the complete nodule

Table 1 Chemical composition of nodules used in this study (BGR samples) in comparison to literature nodule compositions from different regions (wt%)

	BGR samples	Sridhar et al. [16]	Haynes et al. [9]	Han et al. [11]
Mn	31.23	23.20	21.60	20.03
Fe	6.20	6.90	10.4	16.99
Ni	1.36	1.14	0.90	1.26
Cu	1.17	0.80	0.66	0.80
Co	0.16	0.22	0.26	0.37
Mo	0.06	0.06	0.04	0.04
V	0.06	0.04	0.05	n/a
Zn	0.15	0.11	0.11	n/a
Al	2.27	3.07	2.80	2.01
Mg	1.93	1.75	1.53	n/a
Si	5.90	8.60	7.72	8.97
Ca	1.62	1.29	2.12	1.64
Na	2.03	3.80	2.20	n/a
K	0.99	n/a	0.87	n/a
Ti	0.25	0.39	0.73	n/a

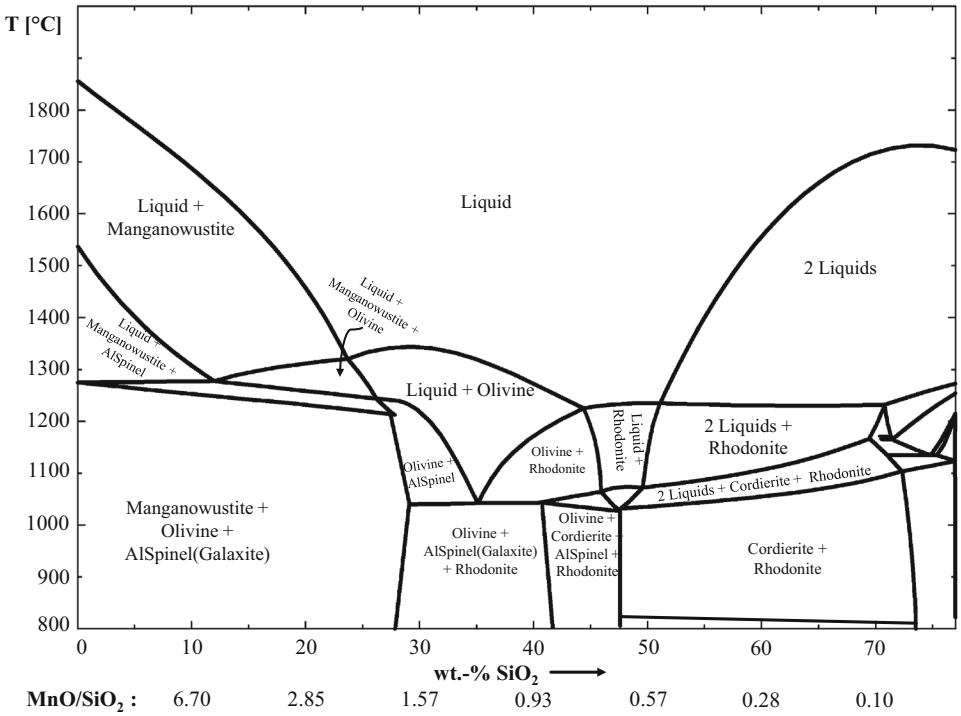

Fig. 2 Quasi binary phase diagram of the five main oxides (MnO, SiO_2, FeO = 12 wt%, Al_2O_3 = 6 wt%, MgO = 5 wt%)

composition (approx. 87 %) and the generalization is therefore somewhat simplified. Nonetheless, the more complete Equilib models in the following section show that an addition of silica meaningfully decreases the slag's liquidus temperature. In these subsequent models, all 15 elements in Table 1 were considered.

FactSage™ Models

Introduction

Thermodynamic models present a great advantage to research of the 1970s and allow the theoretic verification of process routes, which were developed in the past. FactSage™ is a complete thermochemical modeling program with many different applications, e.g., phase diagram calculation, thermodynamic chemical reaction calculations, predominance as well as EpH modeling. The Equilib mode uses Gibbs free energy minimization calculations to simulate the reactions of different reactants to reach a state of chemical equilibrium, and therefore allows the modeling of phase equilibria. It employs a vast variety of thermodynamic databases of pure substances and solutions [22].

The FactSage™ models consider all 15 elements of Table 1 as simple oxides (MnO, FeO, SiO_2, NiO, etc.). Trace elements (<500 ppm) were not taken into account in the calculation to simplify the model. The thermodynamic databases used in the models were:

- FactPS—FACT pure substances database (2013): thermodynamic database for 4776 pure substances
- FToxid—FACT oxide compounds (2013): database for pure oxides and solid as well as liquid solutions
- SGTE—SGTE alloy database (2011): extensive database for alloys and intermetallic phases solid and liquid.

The main disadvantage of this modeling approach is that the solubility of molybdenum trioxide (MoO_3) and vanadium pentoxide (V_2O_5) in the slag phase cannot be modeled, since the FToxid database does not contain data for these compounds. However, FactSage™ allows the creation of ideal solutions from the pure substances database (FactPS). This tool may be used when solution data is missing and the expected concentration of the constituents is dilute. Thus, MoO_3 and V_2O_5 may be modeled as an ideal solution. This solution can then be merged with the slag solution model. Moreover, the complex minerals associated with manganese nodules cannot be modeled in FactSage™, because thermodynamic data for them does not exist. The simplified model of oxides therefore may only allow the deduction of general statements. One should bear in mind that all models have limitations. Nonetheless, the results of the models in this study were verified experimentally.

Model Results

An initial experimental smelting test of the nodules showed that a homogeneous melt could not be obtained in an

electric resistance furnace at a temperature of 1450 °C. Therefore, the FactSage™ "Equilib" model was created to compare the BGR nodules to the studies of Sridhar et al. [16], where a melting range of 1380–1420 °C was postulated. Additionally, the model was used to calculate the liquidus temperature of the slag as a function of MnO to SiO_2 ratio. The results of the simulation are presented in Fig. 3.

Every simulation is based on an input mass of 1000 g of oxides. It is assumed that the nodules are completely moisture free and temperatures are varied according to process parameters. Figure 3 illustrates that an addition of silica decreases the liquidus temperature of the slag up to a MnO/SiO_2 ratio of 1.5. In the calculated phase equilibria, the oxides form a single liquid slag phase with the main constituents MnO and SiO_2.

The main goal of the initial smelting is the phase separation of reduced metal and slag. Therefore, the entire manganese content of the nodules should ideally be separated from the valuable metals in this step. Thus, manganese reduction during the reduction of metal values has to be avoided. Figure 4 shows an activity adjusted Ellingham diagram of the main nodule oxides. The activities of the oxides were obtained from the "Equilib" model of the liquid slag phase. The calculation of the Gibbs free energy (ΔG_R) of the oxidation reaction was carried out in the "Reaction" module of FactSage™ in a temperature range from 1000 to 1700 °C. Strictly speaking, the calculated activities only apply to the liquidus temperature of the slag in the case of no silica addition (1549 °C). However, to get a general impression of the temperature at which the oxides are reduced, this approximation is sufficient.

The diagram signifies that the reduction of manganese(II) oxide may thermodynamically be avoided up to a temperature of approximately 1470 °C. However, the

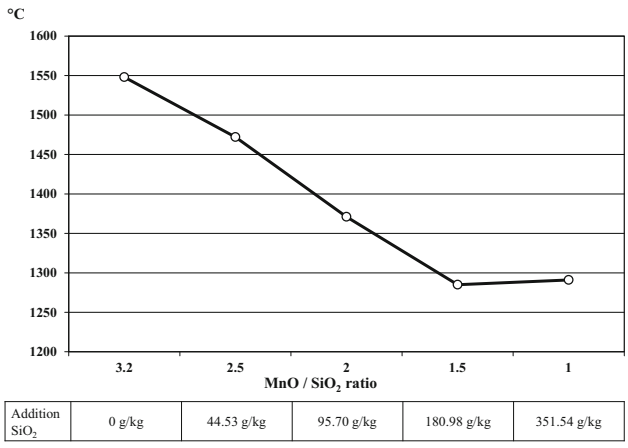

Fig. 3 Correlation between calculated liquidus temperature of the slag phase in the FactSage™ model and SiO_2 addition and resulting MnO/SiO_2 ratio, respectively

reduction of manganese(III) oxide cannot be avoided in the temperature range, where a liquid slag could be obtained. Therefore, a complete separation of manganese from other metal values reduced from the slag is thermodynamically critical. The formation of Mn_2O_3 in the slag cannot be circumvented since a chemical equilibrium between the two manganese oxides always exists. The reduction of iron is thermodynamically impossible to inhibit. Even so, a separation of iron from Ni, Cu and Co would be desirable to avoid additional metal conversion. Vanadium is presented as vanadium(IV) oxide (VO_2) since in the FactSage™ models this vanadium species is the most prominent, even though V_2O_5, V_2O_3 and VO are also considered in the ideal solution approach.

The thermochemical models highlight that the advantages of an adjustment of the MnO/SiO_2 ratio are twofold. The liquidus temperature of the slag is reduced significantly, which reduces energy requirements and wear on furnace refractories. This also allows the metal reduction to be carried out at lower temperatures making the undesired reduction of manganese thermodynamically adverse.

The metal reduction was also simulated using an "Equilib" model in FactSage™. A variable addition of carbon was used as reducing agent. The theoretical stoichiometric amount of carbon necessary to reduce the entire nickel, copper, cobalt, molybdenum and vanadium content adds up to 7.26 g/kg. Therefore, an addition of 29 g(carbon)/kg(oxides), which is roughly the quadruple stoichiometric amount, was simulated. The temperatures at which reduction in the models is carried out are derived from the previously calculated liquidus temperatures plus approximately 100 °C superheat.

The model results for no silica addition ($MnO/SiO_2 = 3.2$, Fig. 5) and a high addition of silica ($MnO/SiO_2 = 1$, Fig. 6) are graphically presented. The comparison of the two cases underlines the positive effects of a precise silica addition on the initial smelting and reduction process step. The decrease in liquidus temperature allows the metal reduction to be conducted at a lower temperature, thus manganese reduction is only significant at a high addition of reducing agent. However, the cases underline that a complete separation of manganese from metal values cannot be achieved thermodynamically. This is, on one hand, due to the reduction of manganese(III) oxide and on the other due to the steady activity increase of MnO during reduction, which is highlighted by the exponential increase of Mn content in the metal phase with excess carbon addition.

Furthermore, the models reveal that the complete reduction of copper is thermodynamically unlikely. However, the reduction is more complete when reduction temperature is lowered (Fig. 6). In the case of no silica addition, only about 90 % of copper can be reduced,

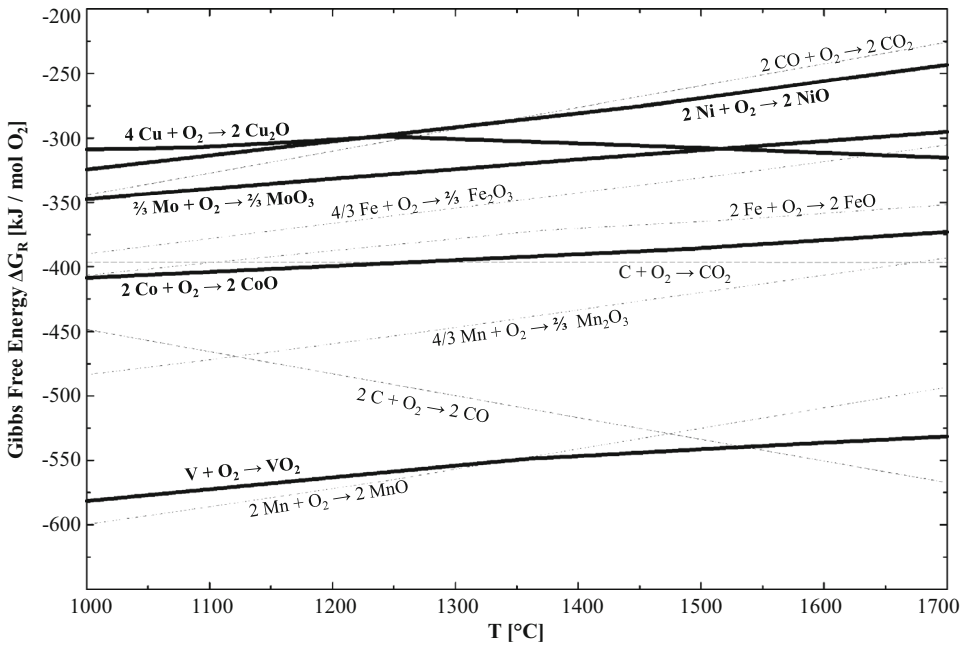

Fig. 4 Activity adjusted Ellingham diagram of the main oxides in the liquid slag. $a(NiO) = 0.0329$, $a(Cu_2O) = 0.0006$, $a(CoO) = 0.0035$, $a(FeO) = 0.1355$, $a(MoO_3) = 0.0005$, $a(Fe_2O_3) = 0.0003$, $a(MnO) = 0.4558$, $a(Mn_2O_3) = 0.0003$, $a(VO_2) = 0.0009$

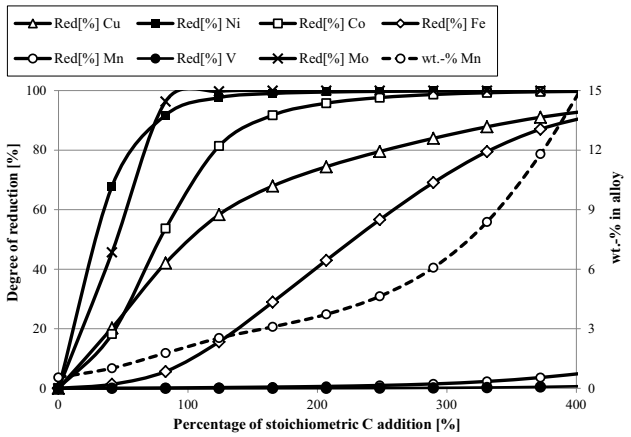

Fig. 5 Simulated carbothermic reduction of metal values from slag with no silica addition ($MnO/SiO_2 = 3.2$) at 1650 °C and resulting Mn content in reduced alloy

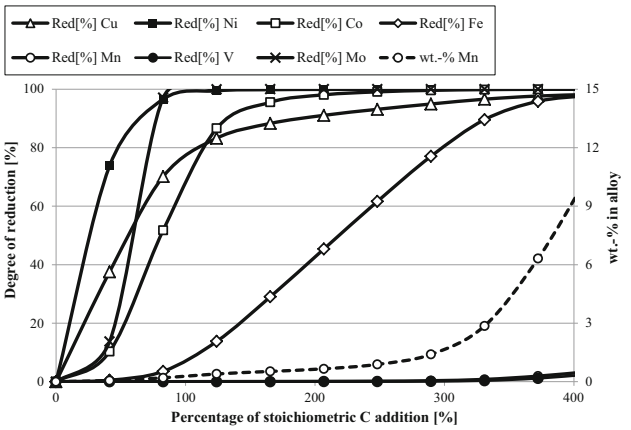

Fig. 6 Simulated carbothermic reduction of metal values from slag with high silica addition ($MnO/SiO_2 = 1$) at 1400 °C and resulting Mn content in reduced alloy

whereas the reduction increases to above 97 % at a MnO/SiO_2 ratio of 1. Contrary to this, the reduction of nickel and cobalt is above 99 % for both MnO/SiO_2 ratios. Molybdenum is also completely reduced from the slag. However, the models show that vanadium may only be slightly reduced, with the assumption that Vanadium behaves ideally, which may only be an approximation of the real chemical behavior.

Kinetic aspects of chemical reactions at high temperatures are not considered in the approach. Similarly, physical metal losses due to incomplete phase separation are not reflected in the models. Additionally, in the models all phases are assumed to be in contact, whereas in reality, phase interfaces have to be considered. The metal recovery in the model therefore represents the maximum recovery theoretically achievable in a state of thermochemical equilibrium.

Nonetheless, the general results from the model are:

- Metal reduction should be carried out at lowest temperature possible
- The initial MnO/SiO_2 ratio should be between 2 and 1
- Control of reduction is critical to attain a low Mn containing metal phase
- Acceptable compromise needs to be found between undesired iron reduction and valuable metal recovery, because iron reduction cannot be avoided.

From the model results the use of an electric arc furnace as proposed by Sridhar et al. [16] seems justified. An EAF could certainly produce the temperatures required for smelting. Additionally, the use of graphite electrodes allows the direct reduction of metals from the liquid slag. Therefore, the furnace should be operated as a submerged arc furnace (SAF), where the electrodes are directly inserted into the slag.

First Lab Scale Verification Experiments

Methods

The practical smelting tests were carried out in a small scale direct current (DC) electric arc furnace. The experimental build-up of the furnace is shown in Fig. 7. The transformer-rectifier has a power output of up to 49 kW with amperage of 120–700 A and a voltage of 24–70 V. The maximum power is infinitely variable. The top electrode position is not automated, but hydraulically positioned by hand. The refractory lining used is an alumina based castable (DIDURIT A87CR-6) manufactured by RHI. It has a high chromium(III) oxide content and is designed for a maximum temperature of up to 1800 °C. This lining proved stable against the slag phase.

In the following section, the results of five experiments are presented and discussed. One experiment was conducted without silica addition, two were done with a MnO/SiO_2 ratio of 1.2 and in two a MnO/SiO_2 ratio of 1 was used. The manganese nodules were ground smaller than 0.5 mm and either pre-reduced at 1100 °C for 3 h or merely dried at 300 °C for 8 h (see Table 2). Due to a limited supply of nodule material additional experiments could not be conducted. But more experimental work is planned in the future.

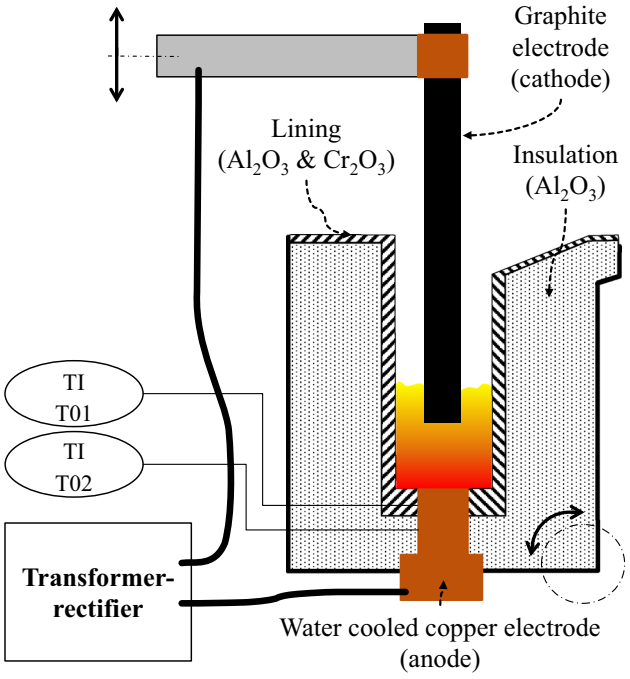

Fig. 7 Schematic layout of the DC arc furnace

The furnace was preheated to approximately 800 °C and then charged with nodules and flux. Approximately 3 kg of material were used per experiment. The reduction time, i.e., the time the electrode was inserted into the liquid slag, was 10 min after all material had been fed into the crucible.

Results and Discussion

The small scale arc furnace experiments prove the key points deduced from the FactSage™ models. Regulating the melt temperature in this experimental build-up is challenging because the top electrode position, and therefore, incoming power is not automated. However, the transformer power was always adjusted so that the melt does not freeze and a homogeneous liquid is obtained. Tapping temperatures in the five experiments were quite similar to the temperatures assumed in the reduction models. In the case of no silica addition (EAF0), the melt temperature was approximately 1600 °C, whereas tapping temperature for the other four experiments was between 1350 and 1450 °C. A picture of the small EAF during tapping of the slag into a steel mold is shown in Fig. 8.

During the experiments slag samples were taken. The first sample was taken after all material had been fed into the crucible and a homogeneous melt was achieved. Additional samples were taken during reduction for two experiments. The slag after tapping was also analyzed. The results, for the reduction of nickel and copper, are graphically presented in the following figures (Figs. 9, 10).

In almost all experiments, the recovery of nickel from the slag into the metal phase was high (above 95 %). The only exception was the trial EAF3 where there was an overall lower metal recovery. The recovery of copper exceeds 85 % during the trials with pre-reduced material. The trials with dried material show lower recoveries for

Table 2 Experimental overview

	Material	MnO/SiO_2
EAF0	Pre-reduced	3.2
EAF1	Pre-reduced	1.2
EAF2	Pre-reduced	1
EAF3	Dried	1
EAF4	Dried	1.2

Fig. 8 Tapping of the slag from the small scale EAF

copper. Higher recoveries should occur, using longer reduction times.

The experiments confirm that reduction of manganese may be minimized through the addition of silica, from the decrease in liquidus, and therefore, reduction temperature. In the trial with no silica addition manganese content of the metal was 34.8 wt%, whereas Mn content in the other four trials lay between 2.8 wt% (EAF2) and 0.1 wt% (EAF1). In all experiments, the Si content in the metal phase was negligibly below 0.1 wt%.

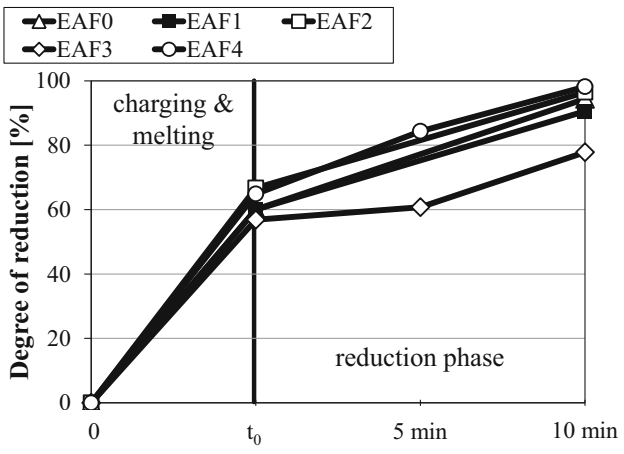

Fig. 9 Carbothermic reduction of Ni from the slag

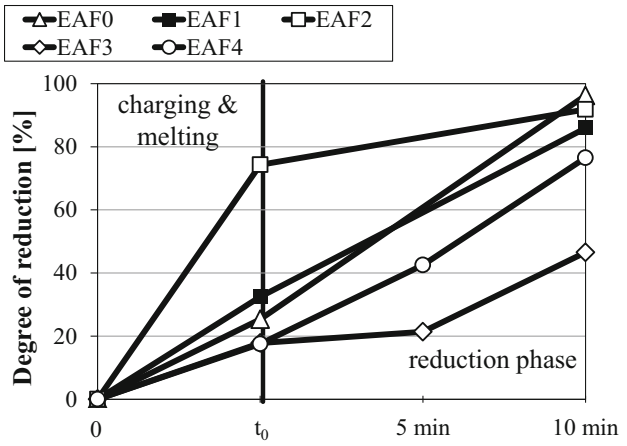

Fig. 10 Carbothermic reduction of Cu from the slag

Figure 11 shows the phase distribution of metal values for the experiment with a MnO/SiO_2 ratio of 1 and pre-reduced nodules (EAF2) in comparison to model results with the same parameters. The values presented are taken for a carbon addition of 200 % (see Fig. 6). The model results are in good accordance with experimental data.

The chemical composition of the experimentally reduced metal at a MnO/SiO_2 ratio of 1 and 3.2 (i.e., no silica flux addition) is given in Table 3. The FactSage™ model predicted values are also indicated. As can be seen in the figure the FactSage™ model predicts the metal composition fairly well. Interestingly, the predicted value for Fe is lower, whereas the values for Ni and Cu are higher. The differences may be due to incomplete activity data in the alloy model, since the database is not specifically tailored to this kind of system. Additionally, the exact amount of carbon consumed cannot be inferred from the experiments, since the electrode also reacts with the atmosphere and not only with the slag. The model predicted an alloy weight of 6.9 % for the metal at a MnO/SiO_2 ration of 1 and of 11.6 % in case of a MnO/SiO_2 ration of 3.2 compared to oxide input weight. The experimentally reduced metal weighted between 7 and 11 % compared to input mass, which corresponds well to the value predicted.

Table 4 shows the slag composition after reduction and the model values are in accordance with the experimental slag composition. The high contents of FeO in the slag for the trial with no flux addition in addition to the relatively high concentration of Ni and Cu suggest that the reduction was incomplete in this trial. Overall, the comparison of Tables 3 and 4 shows that where Fe and Mn content in the metal are higher in the alloy, the contents in the slag are lower as predicted. Therefore, the models are somewhat inconsistent for Fe and Mn reduction and could be optimized. The increased reduction of manganese and iron may

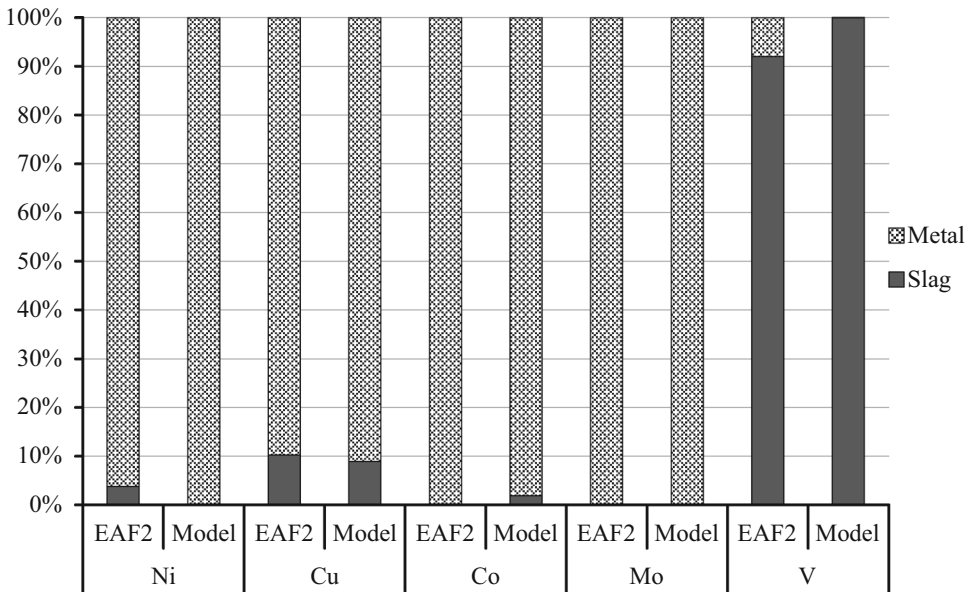

Fig. 11 Phase distribution comparison of EAF2 and model results ($MnO/SiO_2 = 1$, at a carbon addition of 370 %)

Table 3 Comparison of alloy composition in the FactSage™ models and the experimentally obtained metal phases (wt%)

	Fe (%)	Ni (%)	Cu (%)	Co (%)	Mo (%)	Mn (%)
FS $MnO/SiO_2 = 3.2$ @370 %C (1650 °C)	59.1	14.9	11.6	1.8	0.7	11.8
Experimental $MnOSiO_2 = 3.2$ (EAF0)	54.3	13.4	9.1	0.7	0.5	18.5
FS $MnO/SiO_2 = 1$ @370 %C (1400 °C)	63.4	14.5	12.2	1.7	0.6	6.3
Experimental $MnOSiO_2 = 1$ (EAF2)	60.4	17.8	8.4	2.0	0.6	4.1

Table 4 Comparison of final slag composition in the FactSage™ models and the experimentally obtained metal phases (wt%)

	Cu_2O (%)	NiO (%)	FeO (%)	MnO (%)	SiO_2 (%)	Al_2O_3 (%)	CaO (%)	MgO (%)	Na_2O (%)
FS $MnO/SiO_2 = 3.2$ @370 %C (1650 °C)	0.2	0.0	1.6	58.9	19.1	6.5	3.4	4.8	3.5
Experimental MnO- $SiO_2 = 3.2$ (EAF0)	0.7	0.5	9.4	55.3	14.7	4.8	2.6	3.6	2.7
FS $MnO/SiO_2 = 1$ @370 %C (1400 °C)	0.0	0.0	0.4	41.9	42.7	4.5	2.4	3.4	2.9
Experimental MnO $SiO_2 = 1$ (EAF2)	0.2	0.1	3.0	38.0	41.0	2.8	1.9	2.5	2.0

be due to higher Mn_2O_3 and Fe_2O_3 contents in the real operation compared to FactSage™ predictions. Overall FactSage™ modeling proved a reliable tool for slag optimization and reduction predictions in an electric arc furnace for the processing of Mn nodules.

Conclusion and Outlook

The research presented highlights of a sustainable metallurgical process for the treatment of polymetallic deep sea nodules. It was also demonstrated that nodules present a significant resource for nonferrous metals. However, the sustainability of underwater mining remains in question. But the focus of this research aims at the development of a zero-waste, sustainable metallurgical process, and therefore, should be viewed completely detached from the mineral mining. For the first time, thermodynamic modeling of smelting of polymetallic deep sea nodules has been used to set the operating conditions to maximize metal separation and recovery and was verified experimentally. The FactSage™ models allowed the calculation of the liquidus temperatures of the slag, which were close to experimental data, even though some simplifications had to be made in the models. The metal reduction was also successfully modeled in FactSage™ and the results validated in the experiments. Overall, it was demonstrated that through a careful adjustment of the MnO/SiO_2 ratio it is possible to separate most of the manganese content of the

nodules from metal values. The use of an electric arc furnace to melt and separate the two phases has many advantages and could be easily adapted to an industrial scale.

The consideration of the MnO/SiO_2 ratio has proven very useful to characterize a pyrometallurgical process to treat manganese nodules. It is immensely important for a metallurgical process to have a rather unvarying feed material, which is why a target MnO/SiO_2 ratio between 2 and 1 would be ideal. In an industrial process, this could easily be accomplished for each batch of nodules.

The subsequent treatment of the metal phase, however, needs to be studied further. It has to be assessed, if the metal is already marketable or if further processing is necessary. The iron content could quite easily be separated by oxidative converting and silica flux. The following extraction steps as proposed by Sridhar et al. [16] to separate all metal values are challenging from an engineering perspective. Especially, the conversion of the liquid alloy to matte through an addition of elemental sulfur is challenging. Even then, further hydrometallurgical processing is required to extract nickel, copper and cobalt separately. Inserting the converted NiCuFeCo alloy into existing industrial metallurgical routes would be more viable for the processing of ocean nodules.

Therefore, the proposed pyrometallurgical process in two separate electric arc furnace reduction steps to produce NiCuFeCo alloy and ferromanganese is a more sustainable process compared to complex hydrometallurgical and the sulfur route. The disadvantages of all hydrometallurgical routes are mainly the large amounts of acidic tailings (as a Mn product is not generated even though it comprises $\sim$30 wt% of the nodules) and complex solvent extraction processes are necessary due to very low concentrations of valuable metals in solutions. During the first reduction step in the EAF, the valuable metals (Ni, Cu, Co) in comparison are concentrated by a factor >20. Furthermore, a sellable FeMn product may be won from the slag of the first EAF since it is comparable to low grade Mn ores [23]. This reduction process will be subject to further studies. The two-stage reduction offers the possibility of a nearly zero-waste pyrometallurgical process. The resulting slags are a fayalite slag (from alloy conversion), which may also be used in the FeMn reduction step to adjust Fe/Mn ratio, as well as a heavy metal free calcium silicate slag from the ferromanganese reduction EAF. The conditioning of these slags so that they may be useful as cement additions or other construction materials will be subject to future studies. The main goal is the development and experimental verification of a sustainable, zero-waste processing route for polymetallic manganese nodules.

The presence of copper in the final alloy limits the opportunities for the alloy since it may be unsuitable as alloy for the steel or Ni alloy industry. However, further separation of the Cu fraction will be subject to further studies. Due to the uncertain economics of an offshore mining industry [2], the goal for a viable processing option should be the generation of a suitable product, which may be used in existing industries and not the production of grade A metal products.

The main statements from the study are summarized as:

- Liquidus temperature of the slag can be adjusted by decreasing the MnO/SiO_2 ratio
- Favorable ratios were determined to be between 2 and 1
- This decreases the reduction temperature required for the first EAF reduction step
- This allows the near complete separation of the Mn content
- The resulting slag contains (>35 wt% MnO), which should be suitable for FeMn production in a second reduction step
- Lower process temperatures have additional advantages (e.g., lower energy requirements, refractory wear, etc.)
- FactSage™ models showed good compatibility with experiments despite simplifications

Acknowledgments BGR, German Federal Institute for Geosciences and Natural Resources, for the supply of raw nodules and additional support

References

1. Jana RK (1999) Processing of polymetallic sea nodules: an overview. The proceedings of the Third ISOPE Ocean Mining Symposium. International Society of Offshore and Polar Engineers, Goa, India, pp 237–245
2. Lehmköster J, Gelpke N, Visbeck M (2014) World Ocean Review 3: Resources of the sea-chances and risks. maribus gGmbH, Hamburg
3. Senanayake G (2011) Acid leaching of metals from deep-sea manganese nodules—a critical review of fundamentals and applications. Miner Eng 24(13):1379–1396. doi:10.1016/j.mineng.2011.06.003
4. Parhi PK, Park KH, Nam CW et al (2013) Extraction of rare earth metals from deep sea nodule using H_2SO_4 solution. Int J Miner Process 119:89–92. doi:10.1016/j.minpro.2013.01.005
5. Kohga T, Imamura M, Takahashi J et al (1995) Recovering iron, manganese, copper, cobalt, and high-purity nickel from sea nodules. JOM 47(12):40–43. doi:10.1007/BF03221339
6. Pophanken AK, Friedmann D, Friedrich B (2013) Manganese nodules—future resource for technology metals? (Manganknollen—zukünftige Rohstoffbasis für Technologiemetalle?), vol 133. GDMB, pp 1–16
7. Friedmann D, Friedrich B (2015) Pyrometallurgical extraction of valuable metals from polymetallic deep-sea nodules of the German Licensed Territory. European Metallurgical Conference Proceedings. GDMB, Düsseldorf, pp 989–96
8. Halbach P, Friedrich G, von Stackelberg U (1988) The manganese nodule belt of the Pacific Ocean. Ferdinand Enke Verlag, Stuttgart
9. Haynes BW, Law SL, Barron DC et al (1985) Pacific manganese nodules: characterization and processing. Bulletin (United States. Bureau of Mines) 674:43

10. Hubred GL (1980) Manganese nodule extractive metallurgy review 1973–1978. Mar Min 3:191–212
11. Han KN, Fuerstenau DW (1983) Metallurgy and processing of marine manganese nodules. Miner Process Extr Metall Rev 1:1–83. doi:10.1080/08827508308952589
12. Agarwal JC, Wilder TC (1974) Recovery of metal values from manganese nodules. US Patent 3788841
13. Agarwal JC, Beecher N, Davies DS (1976) Processing of ocean nodules: a technical and economic review. J Met 28(4):24–31
14. Han KN, Fuerstenau DW (1975) Acid leaching of ocean manganese nodules at elevated temperatures. Int J Miner Process 2:163–171. doi:10.1016/0301-7516(75)90019-8
15. Cardwell PH, Kane WS (1976) Method for separating metal constituents from ocean floor nodules. US Patent 3950486A
16. Sridhar R, Jones WE, Warner JS (1976) Extraction of copper, nickel, and cobalt from sea nodules. J Met 28(4):32–37
17. Han KN (1997) Strategies for processing of ocean floor manganese nodules. Trans Indian Inst Met 51(1):41–54
18. Cardwell PH (1973) Extractive metallurgy of ocean nodules. Min Congr J 59:38–43
19. Agarwal S, Sahu KK, Jana RK et al. (2009) Recovery of Cu, Ni, Co and Mn from sea nodules by direct reduction smelting. Proceedings of the Eighth ISOPE Ocean Mining Symposium. pp 131–136
20. King D, Pasho DW (1979) A generalized estimating model for the Ocean Management Inc., manganese nodule processing facility—Mineral Policy Sector Internal Report
21. Mohwinkel D, Kleint C, Koschinsky A (2014) Phase associations and potential selective extraction methods for selected high-tech metals from ferromanganese nodules and crusts with siderophores. Appl Geochem 43:13–21. doi:10.1016/j.apgeochem.2014.01.010
22. Bale CW, Chartrand P, Degterov SA et al (2002) FactSage thermochemical software and databases. Calphad 26(2):189–228. doi:10.1016/S0364-5916(02)00035-4
23. Habashi F (ed) (1997) Handbook of extractive metallurgy. Wiley, Weinheim